

1 Chloroplast microsatellites: measures of genetic diversity and the effect of homoplasy

2 M. NAVASCUÉS and B.C. EMERSON

3 Centre for Ecology, Evolution and Conservation, School of Biological Sciences,

4 University of East Anglia, Norwich NR4 7TJ, UK

5

6 *Keywords:* chloroplast microsatellites, genetic diversity, homoplasy, coalescent

7 simulation, conifers

8 Correspondence: Brent Emerson, University of East Anglia, Norwich NR4 7TJ, UK.

9 Telephone: (44) 01603 592237. Fax: (44) 01603 592250. E-mail: b.emerson@uea.ac.uk

10

11 Running title: Chloroplast microsatellite homoplasy

12

13 The definitive version is available at www.blackwell-synergy.com

14 doi: 10.1111/j.1365-294X.2005.02504.x

15

16 **Abstract**

17 Chloroplast microsatellites have been widely used in population genetic studies of
18 conifers in recent years. However, their haplotype configurations suggest that they could
19 have high levels of homoplasy, thus limiting the power of these molecular markers. A
20 coalescent-based computer simulation was used to explore the influence of homoplasy on
21 measures of genetic diversity based on chloroplast microsatellites. The conditions of the
22 simulation were defined to fit isolated populations originating from the colonization of
23 one single haplotype into an area left available after a glacial retreat. Simulated data were
24 compared with empirical data available from the literature for a species of *Pinus* that has
25 expanded north after the last glacial maximum. In the evaluation of genetic diversity,
26 homoplasy was found to have little influence on Nei's unbiased haplotype diversity (H_e)
27 while Goldstein's genetic distance estimates (D^2_{st}) were much more affected. The effect
28 of the number of chloroplast microsatellite loci for evaluation of genetic diversity is also
29 discussed.

30

31 **Introduction**

32 Microsatellites, or simple sequence repeats (SSRs), are sequences of repetitive DNA
33 where a single motif consisting of one to six base pairs is repeated tandemly a number of
34 times. Microsatellite sequences have been identified in the three eukaryote genomes:
35 nucleus, chloroplast (Powell *et al.*, 1995) and mitochondria (Soranzo *et al.*, 1999)
36 Nuclear microsatellite loci are usually highly polymorphic with alleles varying in the
37 number of repeat units; they are codominant and inherited in a mendelian mode. These
38 characteristics, plus being considered selectively neutral, have made them a popular
39 marker for population genetic studies (Sunnucks, 2000). With respect to the organelle
40 genomes, mitochondrial microsatellites have had little impact so far, but chloroplast
41 microsatellites have been increasingly used in population genetics since their discovery.
42 Conserved primers for the amplification of chloroplast microsatellites (cpSSRs) have
43 been reported for conifers (Vendramin *et al.*, 1996), gramineae (Provan *et al.*, 2004) and
44 dicotyledons (Weising & Gardner, 1999), but it is among conifers, for studies of
45 population genetics, that chloroplast microsatellite markers have mainly been used (e.g.
46 Cuenca *et al.*, 2003; Fady *et al.*, 2003; Gómez *et al.*, 2003).

47

48 Chloroplast microsatellites typically consist of mononucleotide motifs that are repeated
49 eight to fifteen times. Levels of polymorphism in cpSSRs are quite variable across loci
50 and across species, and some loci have been found to be monomorphic in all species
51 studied. There are two important features that differentiate chloroplast from nuclear
52 microsatellites. First, chloroplasts are uniparentally inherited. Some species have
53 maternal inheritance of the chloroplast, others paternal. This means that cpSSRs provide

54 information for the lineages of only one of the sexes. Also, the chloroplast chromosome
55 is a non-recombinant molecule and, therefore, all cpSSR loci are linked. The genotyping
56 of cpSSRs will result in haplotypes that will be composed of the combination of alleles
57 found at each cpSSR locus.

58

59 Mutation rates for length variation in microsatellites have been found to be higher (10^{-2} to
60 10^{-6}) than point mutations rates (Li *et al.*, 2002). In order to explain this difference two
61 kinds of mutational mechanism have been proposed: replication slippage (Tachida &
62 Iizuka, 1992) and recombination with out-of-phase aligning (Harding *et al.*, 1992). Both
63 processes result in changes in the number of repeat units which is compatible with the
64 observed size polymorphism of microsatellites. One consequence of these mutational
65 mechanisms is that the same genetic state (i.e. number of repeats) may evolve in two
66 different microsatellite lineages through independent mutational events, a phenomenon
67 known as homoplasy.

68

69 Homoplasy may cause problems in population genetic analysis as it can affect measures
70 of genetic diversity, gene flow, genetic distances (both between individuals and
71 populations), neighborhood size, assignment methods and phylogenetic analysis (see
72 Estoup *et al.*, 2002 for a review). Homoplasy within cpSSRs is considered as a potential
73 limitation for its use as a genetic marker (Provan *et al.*, 2001), however the problem has
74 only been addressed at the genus level (Doyle *et al.*, 1998; Hale *et al.*, 2004). Researchers
75 have generally considered homoplasy levels low enough to allow population genetic
76 analysis, and even when homoplasy has been evident (i.e. a haplotype network with up to

77 nine loops) it has been considered as “moderate” and its potential for confounding results
78 disregarded (Cuenca *et al.*, 2003).

79

80 In the present study, simulation analysis was used to investigate the evolution of cpSSRs
81 in conifers and how homoplasy may influence the informativeness of these markers.
82 Instead of a more traditional simulation approach where the whole population is
83 considered, only the genetic makeup of a sample of individuals was studied, following a
84 coalescence-based approach. The strategy consists of: first, generating a genealogy for a
85 sample of individuals from the last generation; and second, placing random mutations on
86 the genealogy to generate the genetic state of the sample (Hudson, 1990). This approach
87 has proved useful for the study of levels of homoplasy in nuclear microsatellites under
88 different mutational models (Estoup *et al.*, 2002).

89

90 **Modelling chloroplast microsatellite evolution**

91 *Simulation of Coalescent Events*

92 The probability of a coalescent event for any two lineages in a given generation depends
93 on the population size, the population structure and the mating system. Thus, it became
94 necessary to establish the biological scenario of the simulation, which would determine
95 the shape of the genealogy.

96

97 After the last glacial maximum most conifer distributions shifted northward leaving their
98 refugia (Jackson *et al.*, 2000). When populations were established, they had a period of
99 expansion followed by a period of approximately constant population density until the
100 present time (MacDonald & Cwynar, 1991). Our simulations reproduced populations
101 under such conditions. A range of population ages (i.e. coalescence times) were
102 investigated with population origins at 50, 100, 150, 200 or 250 generations before the
103 present to simulate colonization events at different stages of the glacial retreat [assuming:
104 1 generation=100 years (as in Provan *et al.*, 1999) and the last glacial maximum=20
105 000YBP (Hewitt, 1996)]. Population growth was determined by the logistic equation:

106
$$N_{t+1} = N_t e^{r \left(1 - \frac{N_t}{K}\right)} \quad (1)$$

107 where N_t is the population size in the generation t ($N_0=1$), r is the population growth rate
108 and K is the carrying capacity of the population. This model has been widely employed to
109 describe population growth following colonization events (Shigesada & Kawasaki, 1997).
110 The growth rate was set at $r=0.7$, producing a period of expansion with a duration of 22
111 generations (~2200 years), which is within the range observed for *Pinus* (MacDonald &
112 Cwynar, 1991). Then, population size remained constant at carrying capacity for the

113 remaining 28, 78, 128, 178 or 228 generations. Because effective population sizes are
114 considered to be “large” in forest trees (Muona & Harju, 1989), carrying capacity was
115 arbitrarily set at $K=10\ 000$; a size big enough to avoid the effects of genetic drift
116 (Savolainen & Kuittinen, 2000).

117

118 Generally, chloroplasts are considered paternally inherited in conifers, although there is a
119 possibility that low levels of maternal leakage and heteroplasmy may be present (Cato &
120 Richardson, 1996). Thus, the coalescent process influencing the genealogy of chloroplast
121 haplotypes was considered to be the simplest case possible: a neutral, haploid, non-
122 recombinant genome with every individual having the same probability of being the
123 parent of any individual in the following generation. With the demographic history
124 determined, the genealogy was constructed using a generation-by-generation algorithm.
125 This type of algorithm allows the simulation of complex demographic and dispersal
126 models, contrasting with other coalescence algorithms which are faster for computational
127 time (Leblois *et al.*, 2003).

128

129 The algorithm worked backward in time, starting with the last generation and finishing in
130 the first one ($t=0$). In every generation the coalescent events were generated by an
131 algorithm that assigned to every individual, x , from the sample ($x \in [1, \dots, n_t]$) in
132 generation t , its ancestor, y , in the previous generation $t-1$ (Fig. 1). Every individual x
133 from the sample in generation t had a probability $P=n_{t-1}/N_{t-1}$ (where n_{t-1} is the number of
134 ancestors already assigned and N_{t-1} is the population size in generation $t-1$) to share its
135 ancestor y with any of the individuals from the sample which ancestors had already been

136 assigned. A random number, $0 < R < 1$, drawn with a uniform probability distribution
137 function, is used to determine the occurrence of a coalescent event. When $R < n_{t-1}/N_{t-1}$, the
138 ancestor y of the individual x is within the n_{t-1} previously assigned ancestors ($y \in [1, \dots, n_{t-1}]$).
139 In order to determine which ancestor, y took the value of the integer part of $1 + R \cdot N_{t-1}$
140 ($\text{int}(1 + R \cdot N_{t-1}) \in [1, \dots, n_{t-1}]$ when $R < n_{t-1}/N_{t-1}$). The generation and lineages involved in this
141 coalescent event were recorded to construct the genealogy of the sample. When $R > n_{t-1}/N_{t-1}$,
142 the ancestor y was a new individual and y took the value $n_{t-1} + 1$; for the next individual
143 $x + 1$ the value of n_{t-1} increased by one unit.

144

145 Coalescent events were simulated using this algorithm on every generation until all
146 lineages converged to a single lineage. Because the population size in the first generation
147 ($t=0$) is only one individual ($N_0=1$) the probability for any number of individuals to share
148 their ancestors was $P = n_{t-1}/N_{t-1} = 1$, i.e. all the lineages coalesced at least at the first
149 generation. This allowed controlling the coalescence time within the range of time for the
150 phenomenon simulated (i.e. colonization after glacial retreat). It is important to note that
151 due to the non-recombinant nature of the chloroplast genome all cpSSR loci were linked
152 and shared the same genealogical history.

153

154 *Simulation of Mutational Events*

155 Several theoretical mutational models have been proposed to describe microsatellite
156 evolution, each one of them with recognized weaknesses and strengths (Estoup &
157 Cornuet, 1999). All of them refer to, and have been tested against, nuclear microsatellites,
158 where mutational events are believed to occur by two mechanisms: replication slippage

159 and recombination (Li *et al.*, 2002). To our knowledge, no specific model has been
160 developed for cpSSRs (where no recombination occurs) so the stepwise mutation model
161 (SMM) was chosen since it is the simplest realistic model for microsatellites. Mutation
162 rate estimates for cpSSRs are scarce and vary from 10^{-3} (Marshall *et al.*, 2002) to 10^{-5}
163 (Provan *et al.*, 1999) per locus per generation, so simulations were run under four
164 different mutation rates: 10^{-3} , 5×10^{-4} , 10^{-4} , 10^{-5} per locus, per generation.

165

166 The genetic state of nine cpSSR loci in samples of 25 individuals was simulated under 20
167 different combinations of population ages and mutation rates (Table 1). For each of these
168 simulations 20 replicates were run. The output of every replicate consisted of the
169 genotypic information of all the individuals from the sample and the genealogical tree
170 that describe their relationships, with information on the number of mutations and
171 number of generations for every branch. The raw data obtained was analyzed as
172 described in the following section.

173

174 **Genetic diversity analysis**

175 The effect of homoplasmy was studied on a number of standard measures of genetic
176 diversity for cpSSRs: total number of haplotypes, N (direct count of different haplotypes);
177 effective number of haplotypes, N_e (reciprocal of the chance that two randomly chosen
178 alleles are identical); unbiased haplotype diversity, H_e (Nei, 1978), and average genetic
179 distances among individuals, D^2_{sh} (Goldstein *et al.*, 1995) applied to cpSSRs by Morgante
180 *et al.* (1998):

181
$$N_e = 1 / \sum_{h=1}^N p_h^2 \quad (2)$$

182
$$H_e = \left[\frac{n}{n-1} \left(1 - \sum_{h=1}^N p_h^2 \right) \right] \quad (3)$$

183
$$D^2_{sh} = \frac{2}{[n(n-1)]} \cdot \frac{1}{L} \cdot \sum_{i=1}^n \sum_{j=i+1}^n d_{ij}^2 \quad (4)$$

184
$$d_{ij} = \sum_{k=1}^L |a_{ik} - a_{jk}| \quad (5)$$

185 where n is the number of individuals in the simulated sample, p_h is the relative frequency
186 of the h^{th} haplotype, N is the number of different haplotypes in the simulated sample, L is
187 the number of loci simulated, a_{ik} is the size (measured in repeat units) of the allele for the
188 i^{th} individual and at the k^{th} locus, and a_{jk} is the size of the allele for the j^{th} individual and
189 at the k^{th} locus.

190

191 Indices N , N_e and H_e were calculated both for the stepwise mutation model (SMM; where
192 haplotypes were defined by their genetic state) and for the infinite allele model (IAM;
193 where every mutation defined a new haplotype, even if the haplotype produced was

194 already present in the sample). The difference between the SMM and IAM values
195 represents information about genetic diversity that is lost due to homoplasy.

196

197 Estoup *et al.* (2002) defined an index of homoplasy, P , to quantify theoretically the
198 effects of mutational and population variables on homoplasy. This index of homoplasy is
199 the probability that two haplotypes sharing the same genetic state are not identical by
200 descent. We have calculated a similar index generated from Nei's genetic diversity for
201 the SMM and IAM:

$$202 \quad P = 1 - \left(\frac{1 - H_{eIAM}}{1 - H_{eSMM}} \right) \quad (6)$$

203 The number of mutations occurring between every pair of lineages was scored and the
204 average genetic distance, based on number of mutations (D^2_M), was calculated following
205 Equation (4) where d_{ij} is substituted for the number of mutations scored between the
206 individual i and j . Due to the possibility of recurrent mutation and back mutations under
207 the SMM, the genetic distance estimate is expected to be incongruent to some degree
208 with the actual number of mutations between lineages. The differences between the
209 absolute values D^2_{sh} and D^2_M were compared. In addition, the correlation of the matrices
210 of actual and estimated genetic distances was analyzed with a Mantel test (Mantel, 1967)
211 when the difference between D^2_{sh} and D^2_M was large.

212

213 **Results and discussion**

214 The results for all the simulations are presented in Figures 2 and 3. Each of the 20
215 replicates performed for each simulation is equivalent to an independent random
216 sampling from the same population. Hence, for any of the genetic diversity indices, the
217 mean value for the 20 replicates is interpreted as an estimate for the actual population
218 value of that statistic and the standard deviation as the error associated to the sample size
219 used. The effect of sample size was assessed by performing some simulations with larger
220 sample sizes. Not surprisingly this resulted in a reduction of the variance for the different
221 measures; for instance, gene diversity in simulation 16 ($H_{eIAM}=0.552\pm0.178$;
222 $H_{eSMM}=0.542\pm0.178$ for 25 individuals, as shown in Figure 3G; $H_{eIAM}=0.561\pm0.037$;
223 $H_{eSMM}=0.553\pm0.036$ for 1000 individuals) and average genetic distance in simulation 20
224 ($D^2_{sh}=1.665\pm0.382$; $D^2_M=2.746\pm0.706$ for 25 individuals, as shown in Figure 3H;
225 $D^2_{sh}=1.696\pm0.185$; $D^2_M=2.589\pm0.292$ for 1000 individuals). The effect of the sample size
226 could be eliminated by simulating the coalescent history for the whole population.
227 However that would require excessive computational time, and it does not appear to be a
228 problem warranting this.

229

230 As was expected, the simulations with parameters that produced higher genetic diversity
231 also showed higher levels of homoplasy (see Table 1 and Fig. 4). For simulations with
232 mutation rates higher than 10^{-4} , homoplasy caused an underestimation, to different
233 degrees, for the four diversity indices. However, Nei's haplotypic diversity values for
234 SMM and IAM were very close in all simulations.

235

236 In order to understand the effect of homoplasy on Goldstein's genetic distance estimates,
237 a more complex approach is necessary. A difference between the values of D_{sh}^2 and D_M^2
238 will lead to an underestimation of the absolute time of coalescence for that sample.
239 However, the actual and estimated distances between individuals could be correlated, and
240 if that were the case, then the distance estimates could be used, or even corrected, to
241 study relative genetic distances. In order to test that correlation, simulation 20 was chosen
242 as it presents the biggest differences between estimated and actual distances. The Mantel
243 test performed for the correlation of the actual and estimated genetic distance resulted in
244 a significant correlation ($p\text{-value} < 0.025$) for all the replicates, with the correlation
245 coefficient, r , ranging from 0.52 to 0.82. Since the correlation with the actual genetic
246 distances is significant but not predictable, we conclude that, for populations with high
247 genetic diversity, the Goldstein's genetic distance estimates can be misleading, and any
248 attempt to apply a correction to these estimates would be prone to error.

249

250 The different effect of homoplasy on the various indices is explained by the nature of
251 these indices. The three indices based on the number of haplotypes (N , N_e and H_e) seem
252 to perform better for assessing levels of genetic diversity than the one based on distance
253 estimates (D_{sh}^2). Estimated distances are influenced by every parallel mutation and back
254 mutation; however, these mutations may have no influence in the number of haplotypes
255 in the sample. For example, two lineages with unique and parallel mutations will have
256 two distinct haplotypes at the final generation, thus the number of haplotypes will not be
257 reduced. However, the genetic distance will be underestimated because of the parallel
258 mutations. Within the indices based on number of haplotypes, the indices that consider

259 their frequencies (N_e and H_e) were less affected by homoplasy. This result is due to the
260 low frequency that most of the homoplastic haplotypes had within the simulated
261 populations.

262

263 In the present work, methods for phylogenetic reconstruction have not been assessed.
264 However, our results discourage the use of cpSSR to infer phylogenetic relationships. For
265 instance, in simulation 20, the high occurrence of homoplastic mutations (78.8% parallel
266 mutations and 6.4% back mutations) would make parsimony method useless. There
267 would be an effect on distance methods too, because distance estimates are affected by
268 homoplasy. However, further work would be necessary to estimate rates of error.

269

270 The number of cpSSR loci studied also influenced levels of homoplasy. A set of
271 simulations performed for four loci produced higher values for the homoplasy index, P ,
272 and higher differences between expected and actual average distances than the equivalent
273 simulations performed for nine loci (Fig. 4). Thus, the linkage of cpSSRs can be seen as
274 beneficial for the analysis of genetic diversity. With a greater number of loci analyzed
275 one has more power to distinguish haplotypes with homoplastic alleles at a given cpSSR
276 loci through the polymorphism of linked loci.

277

278 Mutation rate and time of coalescence are the two factors influencing the levels of genetic
279 diversity our simulations. The different combinations of these parameters produced a
280 broad range of genetic diversity, from simulation 01 with null diversity to simulation 20
281 with the highest diversity (see Fig. 2 and 3). This set of simulations reproduces the

282 simplest scenario that could describe the recent history of a conifer population: an
283 isolated population originating from a single colonization event, followed by a population
284 expansion. The recent population history of *Pinus resinosa* would seem to be consistent
285 with such conditions. During the last glaciation *P. resinosa* was restricted to southern
286 refugial populations and has colonized northern areas after the glacial retreat (Fowler &
287 Morris, 1977). A study of the population genetics of *P. resinosa* with cpSSRs also
288 supports a metapopulation with restricted gene flow between populations (Echt *et al.*,
289 1998) This case provides us with an empirical study of a conifer with isolated populations
290 and with different colonization ages (either because of the metapopulation dynamics or
291 colonization after glacial retreat). Also, the number of cpSSR loci and sample sizes (nine
292 loci, 21-24 individuals) were similar to the simulations presented here, providing an
293 appropriate combination of conditions for comparison.

294

295 The patterns of genetic diversity found in the empirical study of *P. resinosa* with cpSSRs
296 (Echt *et al.*, 1998) can be best compared with simulations 11-15. In both cases the
297 populations are composed of one high frequency haplotype (the ancestral haplotype in the
298 simulations) plus several low frequency haplotypes. The diversity levels for the different
299 indices, N , N_e , H_e and D^2_{sh} , are also comparable and consistent. Therefore, we can argue
300 that the genetic diversity and distances were unlikely to have been underestimated within
301 *P. resinosa* (see Fig. 2E, 2F, 3E and 3F).

302

303 Any further comparison of our simulations with other conifer species studied with
304 cpSSRs has to be done with caution. The simulations we have performed do not take into

305 account a number of additional factors that may influence homoplasy. Thus the current
306 set of simulations will represent the minimum amount of homoplasy that could be present
307 within a given population. Demographic scenarios including migration or more ancient
308 coalescent events (where colonization events were produced by more than one
309 haplotype), would result in increased levels of homoplasy. Higher mutation rates and size
310 constraints in the mutational model will also increase the levels of homoplasy (Estoup *et*
311 *al.*, 2002).

312

313 To conclude, further simulation studies would be beneficial for the understanding of the
314 homoplasy in the analysis of cpSSRs. In particular, we are now working in the
315 implementation of the generation-by-generation algorithm for the simulation of multi-
316 population scenarios with dispersal that will allow us to understand the effects of
317 homoplasy in the measurement of gene flow and genetic distances among populations.
318 Regarding future empirical studies with cpSSRs, it is strongly recommended that studies
319 use as many cpSSR loci as are available in order to reduce the negative consequences of
320 homoplasy on estimations of genetic diversity. In order to assess levels of genetic
321 diversity Nei's index seems to perform the best, being least affected by homoplasy. In
322 contrast conclusions made with Goldstein's genetic distances should be regarded with
323 caution, as these can underestimate absolute distances.

324

325 **References**

- 326 Cato SA, Richardson TE (1996) Inter- and intraspecific polymorphism at chloroplast SSR
327 loci and the inheritance of plastids in *Pinus radiata* D. Don. *Theoretical and*
328 *Applied Genetics* **93**, 587-592.
- 329 Cuenca A, Escalante AE, Piñero D (2003) Long-distance colonization, isolation by
330 distance, and historical demography in a relictual Mexican pinyon pine (*Pinus*
331 *nelsonii* Shaw) as revealed by paternally inherited genetic markers (cpSSRs).
332 *Molecular Ecology* **12**, 2087-2097.
- 333 Doyle JJ, Morgante M, Tingey SV, Powell W (1998) Size homoplasy in chloroplast
334 microsatellites of wild perennial relatives of soybean (*Glycine* subgenus *Glycine*).
335 *Molecular Biology and Evolution* **15**, 215-218.
- 336 Echt CS, DeVerno LL, Anzidei M, Vendramin GG (1998) Chloroplast microsatellites
337 reveal population genetic diversity in red pine, *Pinus resinosa* Ait. *Molecular*
338 *Ecology* **7**, 307-316.
- 339 Estoup A, Cornuet JM (1999) Microsatellite evolution: inferences from population data.
340 In: *Microsatellites. Evolution and Applications* (eds. Goldstein DB, Schlötterer
341 C), pp. 49-65. Oxford University Press, Oxford.
- 342 Estoup A, Jarne P, Cornuet JM (2002) Homoplasy and mutation model at microsatellite
343 loci and their consequences for population genetics analysis. *Molecular Ecology*
344 **11**, 1591-1604.
- 345 Fady B, Lefèvre F, Reynaud M, *et al.* (2003) Gene flow among different taxonomic units:
346 evidence from nuclear and cytoplasmic markers in *Cedrus* plantation forests.
347 *Theoretical and Applied Genetics* **107**, 1132 -1138.

348 Fowler DP, Morris RW (1977) Genetic diversity in red pine: evidence of low genic
349 heterozygosity. *Canadian Journal of Forest Research* **7**, 343-347.

350 Goldstein DB, Linares AR, Cavalli-Sforza LL, Feldman MW (1995) An evaluation of
351 genetic distances for use with microsatellite loci. *Genetics* **139**, 463-471.

352 Gómez A, González-Martínez SC, Collada C, Gil L, Climent J (2003) Complex
353 population genetic structure in an endemic Canary Island pine using chloroplast
354 microsatellite markers. *Theoretical and Applied Genetics* **107**, 1123-1131.

355 Hale ML, Borland AM, Gustafsson MH, Wolff K (2004) Causes of size homoplasy
356 among chloroplast microsatellites in closely related *Clusia* species. *Journal of*
357 *Molecular Evolution* **58**, 182-190.

358 Harding RM, Boyce AJ, Clegg JB (1992) The evolution of tandemly repetitive DNA:
359 recombination rules. *Genetics* **132**, 847-859.

360 Hewitt GM (1996) Some genetic consequences of ice ages, and their role in divergence
361 and speciation. *Biological Journal of the Linnean Society* **58**, 247-276.

362 Hudson RR (1990) Gene genealogies and the coalescent process. In: *Oxford Surveys in*
363 *Evolutionary Biology Vol. 7* (eds. Futuyma D, Antonovics J), pp. 1-44. Oxford
364 University Press, Oxford.

365 Jackson ST, Webb RS, Anderson KH, *et al.* (2000) Vegetation and environment in
366 Eastern North America during the last glacial maximum. *Quaternary Science*
367 *Reviews* **19**, 489-508.

368 Leblois R, Estoup A, Rousset F (2003) Influence of mutational and sampling factors on
369 the estimation of demographic parameters in a "continuous" population under
370 isolation by distance. *Molecular Biology and Evolution* **20**, 491-502.

371 Li Y-C, Korol AB, Fahima T, Beiles A, Nevo E (2002) Microsatellites: genomic
372 distribution, putative functions and mutational mechanisms: a review. *Molecular*
373 *Ecology* **11**, 2453-2465.

374 MacDonald GM, Cwynar LC (1991) Post-glacial population growth rates of *Pinus*
375 *contorta* ssp. *latifolia* in Western Canada. *Journal of Ecology* **79**, 417-429.

376 Mantel NA (1967) The detection of disease clustering and a generalized regression
377 approach. *Cancer Research* **27**, 209-220.

378 Marshall HD, Newton C, Ritland K (2002) Chloroplast phylogeography and evolution of
379 highly polymorphic microsatellites in lodgepole pine (*Pinus contorta*).
380 *Theoretical and Applied Genetics* **104**, 367-378.

381 Morgante M, Felice N, Vendramin GG (1998) Analysis of hypervariable chloroplast
382 microsatellites in *Pinus halepensis* reveals a dramatic genetic bottleneck. In:
383 *Molecular Tools for Screening Biodiversity. Plants and Animals* (eds. Karp A,
384 Isaac PG, Ingram DS), pp. 407-412. Chapman and Hall, London.

385 Muona O, Harju A (1989) Effective population sizes, genetic variability, and mating
386 system in natural stands and seed orchards of *Pinus sylvestris*. *Silvae Genetica* **38**,
387 221-228.

388 Nei M (1978) Estimation of average heterozygosity and genetic distance from a small
389 number of individuals. *Genetics* **89**, 583-590.

390 Powell W, Morgante M, McDevitt R, Vendramin GG, Rafalski JA (1995) Polymorphic
391 simple sequence repeat regions in chloroplast genomes: applications to the
392 population genetics of pines. *Proceedings of the National Academy of Sciences of*
393 *the United States of America* **92**, 7759-7763.

394 Provan J, Biss PM, McMeel D, Mathews S (2004) Universal primers for the
395 amplification of chloroplast microsatellites in grasses (Poaceae). *Molecular*
396 *Ecology Notes* **4**, 262-264.

397 Provan J, Powell W, Hollingsworth PM (2001) Chloroplast microsatellites: new tools for
398 studies in plant ecology and evolution. *Trends in Ecology & Evolution* **16**, 142-
399 147.

400 Provan J, Soranzo N, Wilson NJ, Goldstein DB, Powell W (1999) A low mutation rate
401 for chloroplast microsatellites. *Genetics* **153**, 943-947.

402 Savolainen O, Kuittinen H (2000) Small population processes. In: *Forest Conservation*
403 *Genetics. Principles and Practice* (eds. Young A, Boshier D, Boyle T), pp. 91-
404 100. CABI Publishing, Oxon.

405 Shigesada N, Kawasaki K (1997) *Biological Invasions: Theory and Practice* Oxford
406 University Press, Oxford.

407 Soranzo N, Provan J, Powell W (1999) An example of microsatellite length variation in
408 the mitochondrial genome of conifers. *Genome* **42**, 158-161.

409 Sunnucks P (2000) Efficient genetic markers for population biology. *Trends in Ecology*
410 *& Evolution* **15**, 199-203.

411 Tachida H, Iizuka M (1992) Persistence of repeated sequences that evolve by replication
412 slippage. *Genetics* **131**, 471-478.

413 Vendramin GG, Lelli L, Rossi P, Morgante M (1996) A set of primers for the
414 amplification of 20 chloroplast microsatellites in Pinaceae. *Molecular Ecology* **5**,
415 595-598.

416 Weising K, Gardner RC (1999) A set of conserved PCR primers for the analysis of
417 simple sequence repeat polymorphisms in chloroplast genomes of dicotyledonous
418 angiosperms. *Genome* **42**, 9-19.
419

420

Acknowledgments

421 We wish to acknowledge the help of Guillermo de Navascués in the program
422 development. We are also grateful to Jo Ridley, Kamal Ibrahim and Godfrey Hewitt for
423 useful comments on early versions of the manuscript. We are grateful to the University
424 of East Anglia for the provision of a PhD studentship to MN.

425

426 **Fig. 1** Coalescence events were simulated with a generation by generation algorithm.
427 This algorithm assigned to every individual, x , of the generation t , its ancestor in the
428 immediately previous generation, $t-1$. The probability for this ancestor to be shared with
429 another individual was calculated from the population size in the previous generation, N_{t-1} ,
430 and the number of ancestors already assigned, n_{t-1} (see text for details).
431

432 **Fig. 2** Number of haplotypes, N , and effective number of haplotypes, N_e , for the 20
433 simulations. Each graph represents the values for one of the indices, N or N_e , for the five
434 simulations with the mutation rate, μ , shown on the left and the coalescence time (in
435 number of generations) shown on the abscissa axis. The mean and standard deviation
436 (from 20 replicates) is shown for each simulation. Both indices were calculated under the
437 stepwise mutation model (SMM) and the infinite allele model (IAM). The difference
438 between both values represents the extent to which information is lost due to homoplasy.
439

440 **Fig. 3** Unbiased haplotype diversity, H_e , and average genetic distances among
441 individuals, D^2 , for the 20 simulations. Each graph represents the values for one of the
442 indices, H_e or D^2 , for the five simulations with the mutation rate, μ , shown on the left and
443 the coalescence time (in number of generations) shown on the abscissa axis. The mean
444 and standard deviation (from 20 replicates) is represented for each simulation. H_e was
445 calculated for the stepwise mutation model (SMM) and the infinite allele model (IAM).
446 D^2 was calculated for estimated distances (D^2_{sh}) based on the number of observed
447 mutations and for the true distances based on the actual number of mutations (D^2_M). The
448 difference between both values represents the extent to which information is lost due to
449 homoplasy.

450

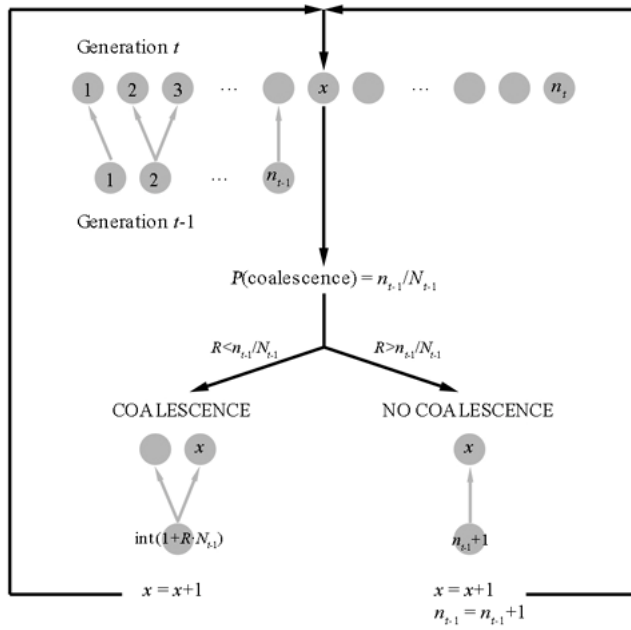
451 **Fig. 4** Levels of homoplasy plotted against genetic diversity for every replicate of the 20
452 simulations (see Table 1 for simulation conditions). Levels of homoplasy are represented:
453 (A) with the homoplasy index, P , and (B) with the difference between the actual average
454 genetic distance (D^2_M) and the estimated genetic distance (D^2_{sh}). Filled circles represent
455 simulations with nine loci and empty circles represent equivalent simulations with only
456 four loci.
457

458 **Table 1** Combinations of parameters for coalescence time and mutation rate used in
 459 different simulations, and the index of homoplasy found for each.

	Coalescence time ^a	Mutation rate, μ	Homoplasy index, P^b
Simulation 01	50	10^{-5}	0.00
Simulation 02	100	10^{-5}	0.00
Simulation 03	150	10^{-5}	0.00
Simulation 04	200	10^{-5}	0.00
Simulation 05	250	10^{-5}	0.00
Simulation 06	50	10^{-4}	0.00
Simulation 07	100	10^{-4}	0.00
Simulation 08	150	10^{-4}	0.00
Simulation 09	200	10^{-4}	0.00
Simulation 10	250	10^{-4}	0.00
Simulation 11	50	5×10^{-4}	0.01
Simulation 12	100	5×10^{-4}	0.03
Simulation 13	150	5×10^{-4}	0.03
Simulation 14	200	5×10^{-4}	0.07
Simulation 15	250	5×10^{-4}	0.17
Simulation 16	50	10^{-3}	0.02
Simulation 17	100	10^{-3}	0.06
Simulation 18	150	10^{-3}	0.11
Simulation 19	200	10^{-3}	0.33
Simulation 20	250	10^{-3}	0.43

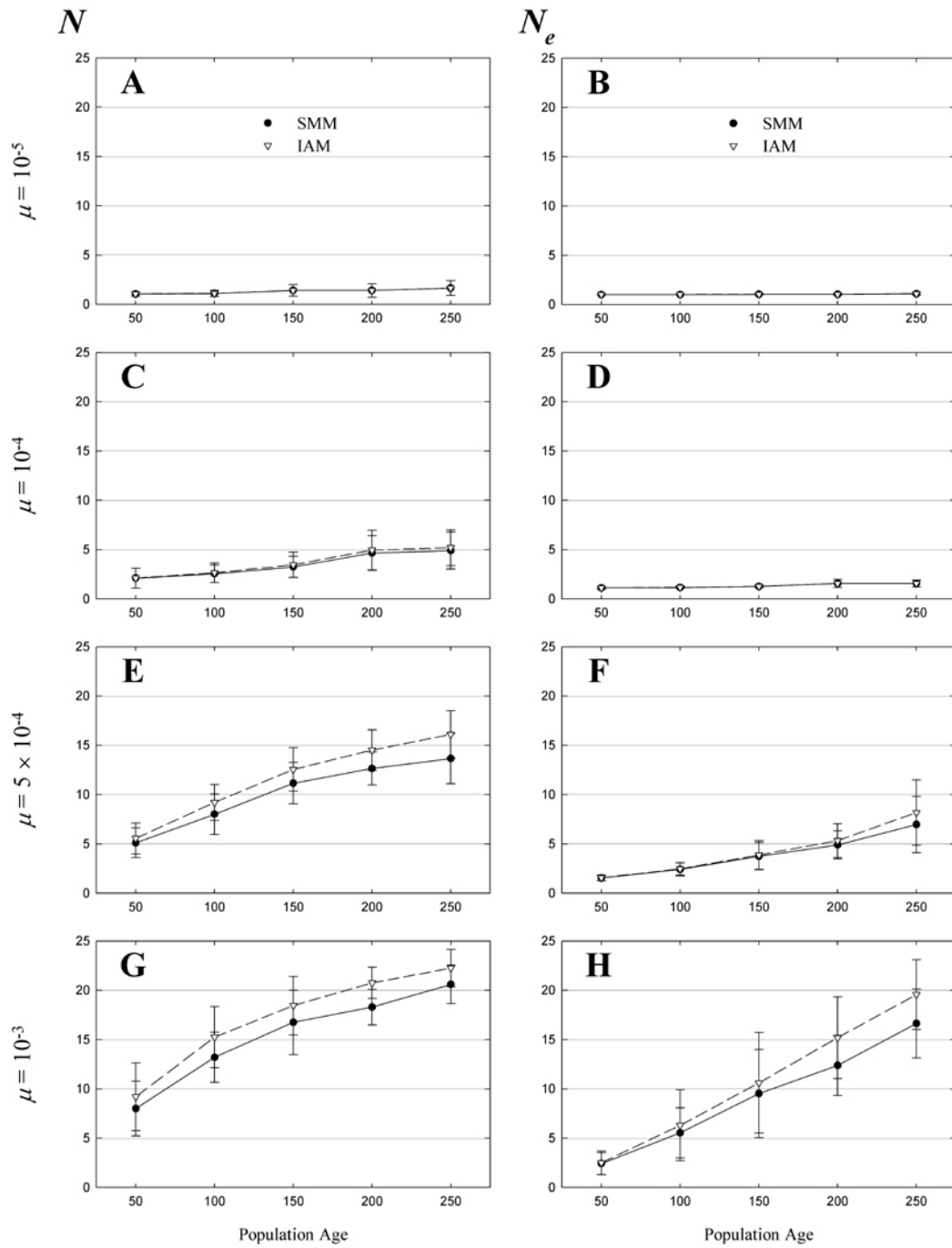
460 ^a coalescence time in number of generations; ^b mean from 20 replicates

461



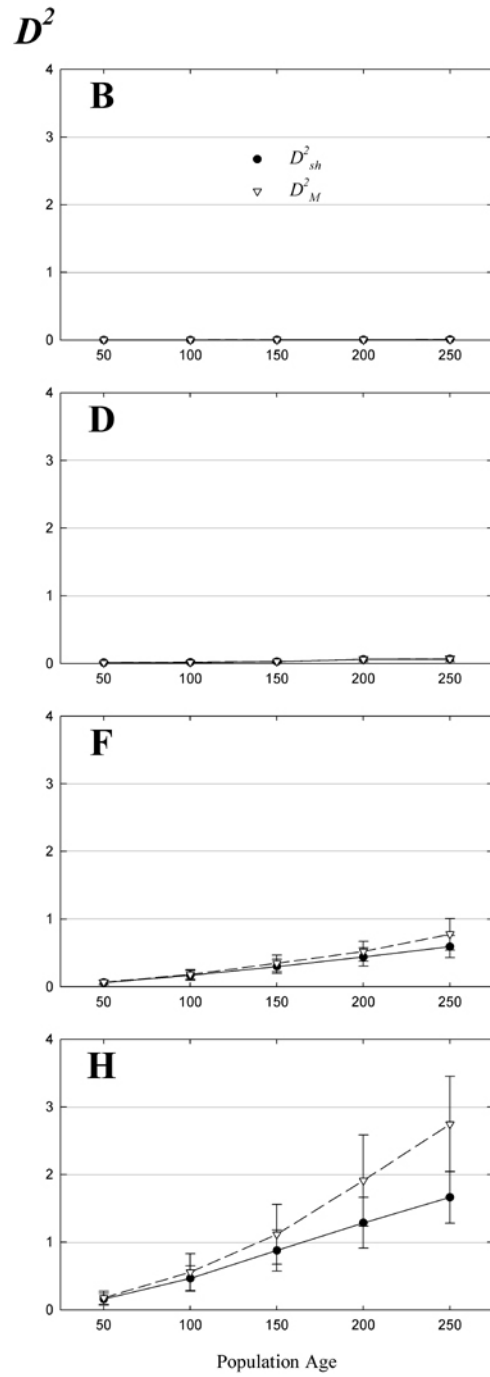
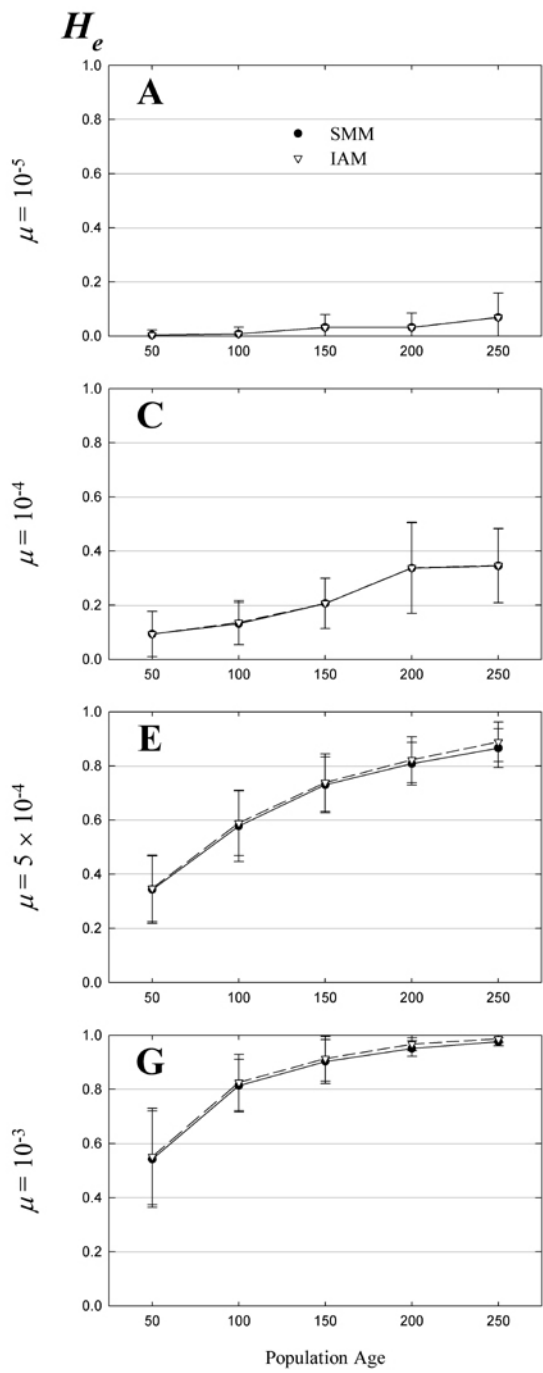
462

463



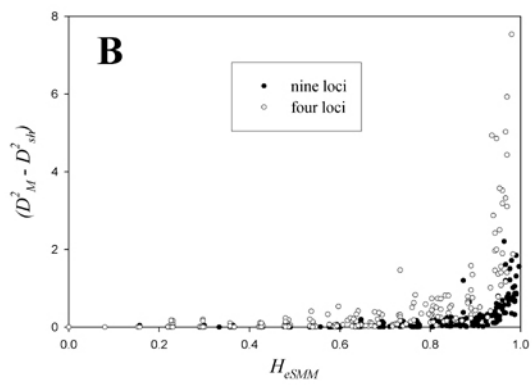
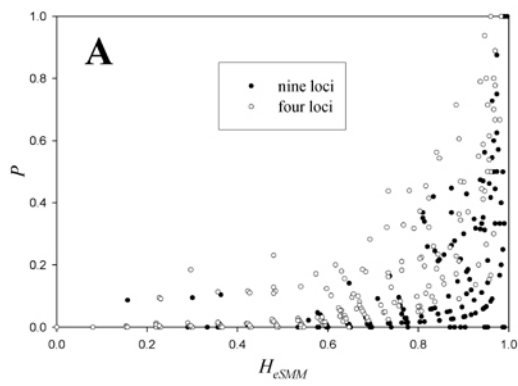
464

465



466

467



468